Tailoring One-dimensional Assemblies of Chiral Bowl-shaped Molecules with Diverse Enantiomers and Polar Column Alignments

Dan He,[1,2‡] Barun Dhara,[1‡*] Cheng Zhang,[1,3] Atsuko Nihonyanagi,[1] Hiroyuki Inuzuka,[1] Eiju Hara,[4] Shunsuke Sato,[4] Kiyohiro Adachi,[5] Go Watanabe,[4,6,7*] Daisuke Hashizume,[5] Kou Okuro,[8] and Daigo Miyajima[1,9*]

[1]*RIKEN Center for Emergent Matter Science, 2-1 Hirosawa, Wako, Saitama 351-0198, Japan*

[2]*College of Chemistry and Chemical Engineering, Central South University, Changsha 410083, P. R. China*

[3]*Key Laboratory of Green Chemistry and Technology of Ministry of Education, College of Chemistry, Sichuan University, Chengdu 610064, P. R. China*

[4]*Department of Physics, School of Science, Kitasato University, Sagamihara, Kanagawa, 252-0373 Japan*

[5]*Materials Characterization Support Team, RIKEN Center for Emergent Matter Science (CEMS), 2-1 Hirosawa, Wako, Saitama, 351-0198, Japan*

[6]*Department of Data Science, School of Frontier Engineering, Kitasato University, Sagamihara, Kanagawa 252-0373, Japan*

[7]*Kanagawa Institute of Industrial Science and Technology (KISTEC), Ebina, Kanagawa 243-0435, Japan*

[8]*Department of Chemistry and State Key Laboratory of Synthetic Chemistry, the University of Hong Kong, Pokfulam Road, Hong Kong, R. R. China*

[9]*School of Science and Engineering, the Chinese University of Hong Kong, Shenzhen 518172, P. R. China*

Symmetry is an important factor in material design. Generally, it is difficult to quantitively discuss symmetry-property relations. Two materials only with symmetry differences are requisite to verify whether polar or nonpolar chiral systems are advantageous for a specific property/phenomenon, such as chirality-induced spin selectivity. However, it is difficult to selectively prepare materials having different symmetries without changing other physical properties. The current study successfully prepared seven exceptionally similar crystals with different symmetries in terms of polarity, chirality, and enantiomer alignments, which affords ideal materials for the abovementioned studies. Furthermore, we revealed a universal guiding principle on the self-assembly pattern of bowl-shaped molecules to predict the resultant assembled structures with the help of molecular dynamics simulations.

Physical properties of materials are qualitatively decided by their symmetries. For example, ferroelectricity can be observed only in materials with polar point group symmetry. In addition, the recent, well-discussed bulk photovoltaic effect (BPVE) and chirality-induced spin selectivity (CISS) are observed in materials with noncentrosymmetric[1-3] and chiral point group symmetry.[4-7] Although such symmetry constraints, necessary to realize certain properties/phenomena, are widely recognized, it is always unclear how other symmetry components affect the corresponding properties/phenomena. To the best of our knowledge, it is not unveiled that whether chiral and polar systems can have a larger CISS effect than chiral and nonpolar systems. Thus, materials with different symmetries but nearly identical parameters should be studied. For example, given that chiral bowl-shaped π-conjugated molecules are stacked straight forming a two-dimensional (2D) assembly, eight assemblies with different symmetries can be considered (Figure 1). They are labeled according to their asymmetric elements: (i) polar and enantiomeric (P/E, ①), (ii) nonpolar and enantiomeric (N/E, ②), (iii) polar and racemic-segregated (P/Rs, ③), (iv) nonpolar and racemic-segregated (N/Rs, ④), (v) polar and racemic-alternating (P/Ra, ⑤), (vi)

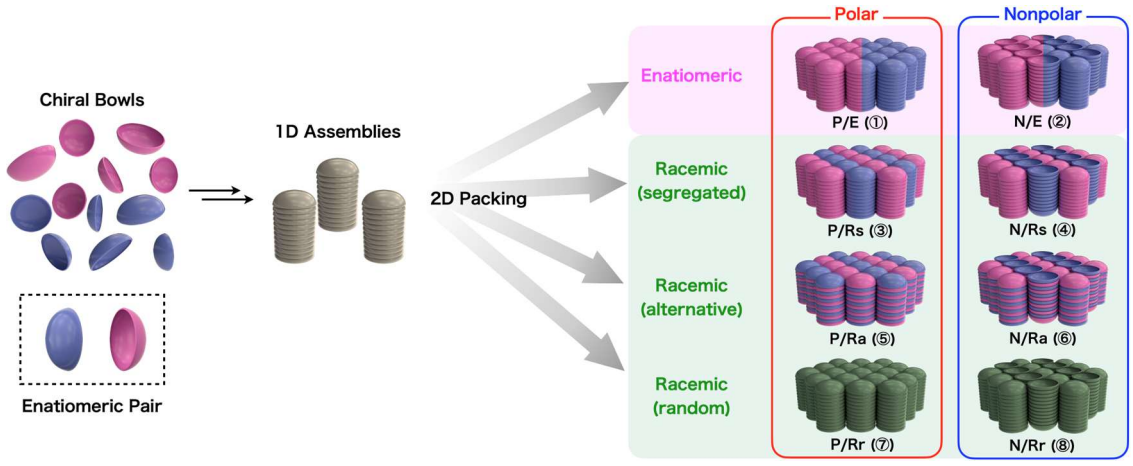

Figure 1. Schematic illustration of possible two-dimensional packings of columns consisting of chiral bowl-shaped molecules.

nonpolar and racemic-alternating (N/Ra, ⑥), (vii) polar and racemic-random (P/Rr, ⑦), and (viii) nonpolar and racemic-random (N/Rr, ⑧). If we thoroughly examine all the substances that have been reported, molecular assemblies with similar symmetries to these eight kinds might be recorded for each of them.[8, 9] However, the impact of symmetry on physical properties cannot be discussed if their molecular structures are significantly different. If these molecular assemblies can be individually prepared by minimizing the modification of their molecular structures, it provides design guidelines to enhance properties/phenomena, such as CISS and BPVE. The present study demonstrated that seven of the eight structures could be individually synthesized by changing the size and position of halogens. Furthermore, the revealed self-assembling rule of bowl-shaped molecules and molecular dynamics (MD) simulations were combined to propose a simple method to predict these assembled structures.

Results and discussion

Recently, the introduction of three or more fluorine (F) atoms at the α-positions of subphthalocyanine (SubPc), a bowl-shaped π-conjugated molecule, forms polar structures with trigonal lattices (① and ⑦, Figure 1) while introducing F at the β-positions of SubPc forms nonpolar structures (② and ⑧).[10] In the present study, similar SubPc derivatives were synthesized, where chlorine (Cl), bromine (Br), and iodine (I) is introduced in place of F (Supporting Information Part S2 and S3), while analyzing the crystal structures of these derivatives. The synthesized eight SubPc derivatives all possess chiral C_3-symmetry (Figure 2). We prepared and characterized 16 crystals with their enantiomers and racemic mixtures. The racemic mixtures afford the crystals of the corresponding racemates, indicating no chiral resolution. Note that the four F-based SubPc crystals in this study have

been reported in our previous study.[10]

The space groups of 16 crystal structures are summarized in Table 1 (the details are presented in Table S3 and Figures S25–S36). The obtained crystal structures are classified into eight assemblies in Figure 1 and illustrated in Figure 3 (The schematic illustrations of *R*3*m* and *C*2 are included in Supplementary, since *R*3 and *R*3*m*, and $P2_1$ and *C*2 are similar). Figure 3 shows that SubPc stacks straight across all crystals. A limited number of structures form one-dimensional (1D) assemblies in crystal structures among the reported bowl-shaped π-conjugated molecules.[11-14] Moreover, even fewer cases exhibit straight stacking. On the other hand, if bowl-shaped molecules stack in a zigzag manner, material properties would be differentiated depending on their zigzag manners. Hence, the straight-stacked bowls simplify the quantitative discussion of the effects of symmetry elements, such as chirality and polarity, on the physical properties of crystals.

The structures are color-coded to classify the obtained crystal structures based on polarity (Table 1). Red represents polar structures with SubPc columns in a parallel alignment, while blue represents nonpolar structures with SubPc columns in an antiparallel alignment. Green represents polar structures, but methanol (MeOH), utilized for crystallization, is arranged as 1D channels. SubPc columns are assembled into trigonal lattices except for two crystals ($Pna2_1$) which are color-coded as pale red. Except for $P2_1/c$ (pale blue), the space group of nonpolar structures is $P2_12_12_1$.

The effects of chirality and halogens on the assembling patterns of SubPc have been discussed. Two enantiomers are randomly arranged in F-containing crystals. No

difference exists in the assembling patterns between the crystals with pure enantiomers and racemic mixtures. Meanwhile, the assembling patterns of Cl-, Br-, and I-containing crystals differ between enantiomers and racemic mixtures.[12, 15, 16] In general, the crystal structures between enantiomers and racemic mixtures are different.[12, 17] Hence, the formation of the same structures between enantiomers and racemates by the SubPc-3F series is an exception. F is a halogen with the smallest size. When the two enantiomers are interchanged, the influence on packing must be the smallest. The random arrangement of the two enantiomers is entropically favorable.

Crystals with the 1D assembly of chiral bowl-shaped molecules are classified into eight groups based on chirality, polarity, and enantiomer alignments. Table 1 shows that SubPc derivatives with different halogen substituents form seven of the eight groups (except for ⑥). These results indicate that the exceptionally similar assemblies can be individually synthesized by introducing minimal changes in the molecular structure of SubPc. The physical properties of these obtained crystals should be different due to the halogen difference. However, absorption profiles remain nearly unchanged with different halogen substituents (Figure S17), due to the fact that halogens contribute little to the highest occupied molecular orbital (HOMO) and lowest unoccupied molecular orbital (LUMO). Density functional theory calculations revealed that HOMO–LUMO orbitals are hardly

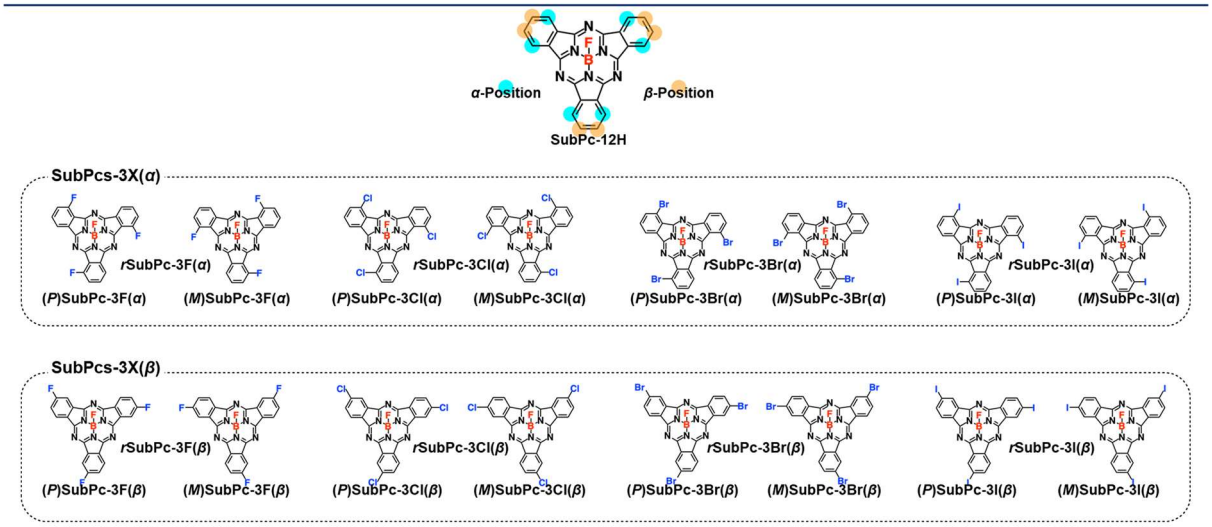

Figure 2. Chemical structures of chiral subphthalocyanine (SubPc) derivatives together with a schematic illustration of the α- and β-positions of SubPc.

localized on halogens (Figure S18). Alternately, the absorption maximums of SubPc with halogens at α-positions are slightly red-shifted from those with halogens at β-positions. As far as different molecules are used, various properties will inevitably be altered. To the best of our knowledge, there are no similar examples where the symmetry of molecular assemblies is distinguished using similar molecules. These are the ideal samples to investigate the correlation between symmetry and physical properties.

Table 1. The summary of the space groups of SubPc derivatives. ①–⑧ correspond to the molecular arrangements discussed in Figure 1.

	α		β	
	Enantiopure	Racemic	Enantiopure	Racemic
F	*R*3(①)	*R*3m(⑦)	$P2_12_12_1$(②)	$P2_12_12_1$(⑧)
Cl	$P2_12_12_1$(②)	*R*3c(⑤)	$P2_1$	$P2_1/c$(④)
Br	$P2_12_12_1$(②)	*R*3c(⑤)	$P2_1$	$Pna2_1$(③)
I	$P2_12_12_1$(②)	*R*3c(⑤)	*C*2	$Pna2_1$(③)

Polar (parallel) / Non-Polar (anti-parallel) / Polar (parallel) with MeOH

The SubPc molecules stack straight in all the crystals of this study, minimizing the influence of local molecular arrangements. They are highly suitable for comparing the symmetry of arrangements, including polarity and chirality. MeOH molecules are arranged to form 1D channels in (*P*)SubPc-3Cl(β), (*P*)SubPc-3Br(β), and (*P*)SubPc-3I(β) crystals. A chiral, polar, and porous structure promising various applications, such as optical separation and asymmetric synthesis, can be obtained by removing MeOH without disturbing the assembly pattern of SubPc molecules. However, in our preliminary trials, the assembly pattern of SubPc is drastically altered when MeOH is removed by heating the crystals under a vacuum. On the other hand, multistep solvent exchange techniques might remove solvent molecules from porous assemblies without losing their original structures.[18, 19] Thus, careful handling may achieve a chiral, polar, and porous structure even in our system.

We successfully designed the molecular assemblies with different symmetry patterns through minimal changes to their molecular components. However, it is desirable to predict the assembly patterns of the synthesized molecular structures in material design. Hence, we considered a possible guiding principle to govern the assembling pattern of the examined SubPc derivatives. Upon observing the correlation between the obtained crystals and their molecular assemblies, we noticed that the key element, governing the assembling patterns of SubPcs, can divide the obtained crystals into two major categories (orange and

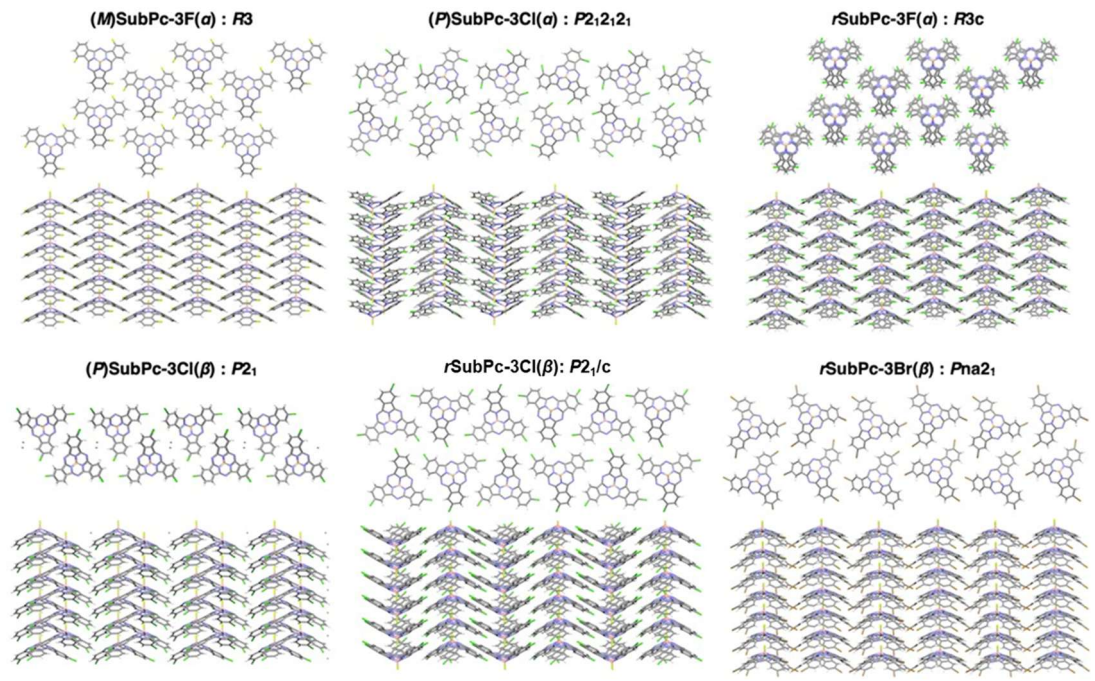

Figure 3. Schematic illustrations of representative molecular packings of SubPc derivatives. Other crystals are summarized in Figure S37.

white cells in Table 1). The crystals in orange cells are either polar crystals with a trigonal lattice or nonpolar crystals with the space group of $P2_12_12_1$. In contrast, the crystals in white cells exhibit other structures. This distinction is not only based on the crystal symmetry but also our observation during the experiments to prepare single crystals. Specifically, the crystals in the orange cells could be prepared by adding a poor solvent, such as MeOH, to chloroform or chloronaphthalene solutions. Their crystallization conditions had to be optimized for each case (Table S2). Considering these experimental differences, we investigated the characteristic differences between the molecules of the orange and white cells in their self-assembling patterns. We hypothesized that the molecular shape differentiates the assembling principle between the orange and white cells. Based on the obtained crystal data, the eight SubPcs used in this study were depicted with space-filling models (Figure 4). Although the SubPc derivatives appear to have similar shapes at a glance,

the shapes of SubPc derivatives in orange cells are close to a circle. In contrast, those in white cells deviate from a circular shape with increasing halogen size (Figure 4). The dense packing of molecules during their assembly is thermodynamically preferable. Hence, 1D assemblies of SubPc derivatives prefer to assemble into close-packed structures whenever feasible. As the shape of SubPc derivatives gets close to circular ones, the cross-section of the corresponding 1D assemblies also becomes circular, forming close-packed structures. The obtained trigonal lattices are closed-packed (Figure 3). In contrast, $P2_12_12_1$ structures are not closely packed due to their symmetry. However, their 2D arrays resemble a close-packed structure (Figure 3). In fact, their packing densities are nearly identical to those of the corresponding trigonal lattices [e.g., the densities of (*M*)SubPc-3Cl(α) and *r*SubPc-3Cl(α) crystals are 1.624 and 1.645 g cm^{-3}, respectively, Table S3]. Hence, we consider that, in this system, $P2_12_12_1$ is a kind of closed-packing for antiparallel arrays of 1D columns. The difference between the SubPc derivatives in orange and white cells (Figure 4) indicates a tendency for molecules with halogens at the α- and β-position to be classified as orange and white, respectively. Considering the fact that SubPc-3F(β)-based crystals are classified into orange, we concluded that the molecular shape is a major determining factor in the 2D packing of columns. Multiple 2D packing possibilities with similar energy levels arise as the cross-section of the SubPc column deviates from a circular shape. Such systems cannot converge to a single assembly, making it difficult to obtain single crystals. This assumption is supported by the fact that (*M*)SubPc-3Br(β) and (*M*)SubPc-3I(β) are differently packed despite the small differences in the halogen sizes. The most stable packing would change with a small alteration of molecular structures, due to the different packing patterns with

similar thermodynamic stability. Although the above discussion is estimated from the results only with SubPcs, the obtained guiding principle is based on the molecular shapes and must be universal for all bowl-shaped π-conjugated molecules.

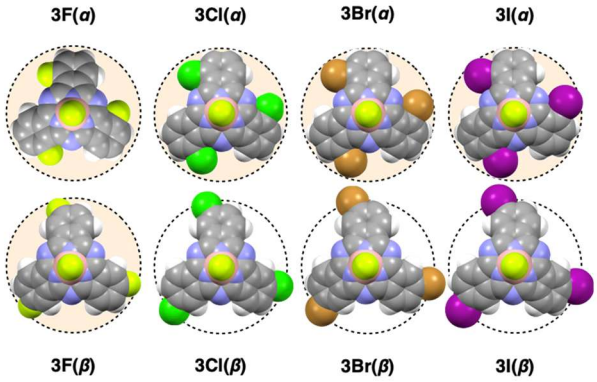

Figure 4. Top-view images of SubPc derivatives based on their corresponding single crystal data. The same dashed circular lines, corresponding to the peripheral of non-substituted SubPc, are placed to compare the sizes. SubPcs on top of orange circles correspond to the crystals in orange cells in Table1.

The packing of SubPc derivatives with halogens at β-positions is difficult to predict. However, they form diverse packing patterns that cannot be obtained using simple close-packed arrangements. Alternately, circular-shaped SubPc derivatives would adopt either a trigonal or $P2_12_12_1$ structure. This alone is an important guideline for material design, but ideally, we would like to perfectly predict whether it will form a polar or nonpolar structure, in other words, whether it will adopt trigonal or $P2_12_12_1$. In our previous studies, the formation of polar or nonpolar assemblies of F-substituted SubPc derivatives could be predicted through MD simulations.[10] Herein, we further investigated whether MD simulations could be applied to SubPc derivatives substituted with different halogens than

F. However, predicting the molecular assembly pattern is difficult, since it requires simulating all the possible assembled patterns while comparing their energy levels. We narrowed down the structures to $P2_12_12_1$ and trigonal, which made it feasible to accurately compare the energy of both structures. *R*3*c* and $P2_12_12_1$ structural formation using (*M*)SubPc-3Cl(α) were compared through MD simulation (Figure 5a) to confirm whether the experimentally obtained crystal structure ($P2_12_12_1$) was energetically more favorable than *R*3*c* that could not be obtained. For the assembly structures that were not actually obtained, molecular assemblies obtained from other molecules were used as the initial structures, followed by optimization. For example, the molecular assemblies of *r*SubPc-3Cl(α) were utilized as the initial structures for trigonal assemblies of (*M*)SubPc-3Cl(α). Although these initial structures should be slightly different from the optimal trigonal structure of (*M*)SubPc-3Cl(α), molecules can move and change their configurations during simulation from the initial structure. MD simulations can provide the total energy of the resultant assemblies as well as the magnitude of molecular fluctuations as the *B*-factor (temperature factor or Debye-Waller factor)[20] used for color coding. *B*-factor is commonly used to represent the thermal fluctuations of atoms in the MD simulations of proteins, where blue and red indicate less and larger fluctuation, respectively. As shown in Figure 5, the fluctuation (red parts) of SubPc for the experimentally "NOT"-obtained structures becomes unevenly large with increasing temperature, which indicates that the assembly structure is distorted and not a stable packing. The total energy of the assembled structures confirms the higher stability of the experimentally obtained crystal structure (Table S4). Although the total energy of structures indicates their stability, the *B*-factor allows us to understand the

reason intuitively. Furthermore, the simulation results of *r*SubPc-3Cl(α), (*M*)SubPc-3Br(α), and *r*SubPc-3Br(α) (Figures 5b, S38a, and S38b) all well reproduced the experimental results. Thus, at a minimum computational cost, molecular design guidelines can accurately predict three-dimensional assembly structures (trigonal or $P2_12_12_1$).

Finally, the importance of the straight 1D array of SubPc derivatives in the obtained crystals was studied. The eight types of possible 2D arrays of SubPc columns are presented in Figure 1, while they cannot be simplified such that if SubPcs stack with a zigzag pattern. One may imagine that bowl-shaped molecules are easily stacked up straight. In fact, most bowl-shaped molecules present herringbone structures with CH–π interactions stabilizing the formed assemblies.[21-26] For example, nonsubstituted SubPc forms the herringbone structure.[27] Therefore, our results could indicate that replacing peripheral

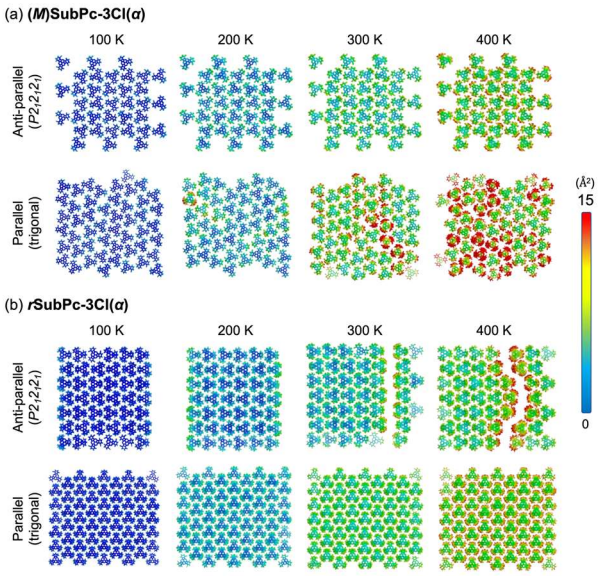

Figure 5. Color-coded *B*-factor distributions (Å^2) obtained from MD simulations for (a) (*M*)SubPc-3Cl(*α*) and (b) *r*SubPc-3Cl(*α*). The magnitude of *B*-factors is represented by the color-coded scale bar.

hydrogens of bowl-shaped molecules with halogens suppresses CH–π interactions. This enhances the possibility of forming a straight 1D array of the resultant bowl-shaped molecules. Similar examples are also reported with the other bowl-shaped π-conjugated molecules.[28] Corannulene, a partial fullerene structure, does not form a 1D assembly in its crystal structure.[29] However, its halogen-substituted derivatives form 1D stacks in its crystal structures.[30-33] Hence, halogen substitution could be a universal design principle for bowl-shaped molecules to form straight 1D assemblies. The conductivity of the obtained crystals is quite low and not applicable for studying the CISS effect. Currently, we are trying to prepare thin films of the studied crystals.

Conclusions

C$_3$-symmetric SubPc derivatives successfully tailored exceptionally similar 1D assemblies with different symmetries based on chirality, polarity, and enantiomer alignment. Although eight different SubPc derivatives were used to form seven different assembly patterns, the physical properties of the molecules remained similar. Therefore, the developed systems are ideal for studying the quantitative correlation between symmetry and property. Furthermore, we unveiled the universal guiding principle that circular- and bowl-shaped π-conjugated molecules preferred to assemble into closed-packed-like structures, enabling the prediction of resultant assembled structures. Despite the large number of studies on the relationship between molecular structure and its packing, there remains a dearth of reports that have led to the point of proposing universal guiding principles. The crystals and design principles obtained are expected to open new avenues for materials science.

Additional Information

Supporting information contains materials and methods, synthetic procedures, experimental details, NMR, Mass, UV-absorption, CD, crystallographic data of all compounds and theoretical calculations.

CCDC 2306958, 2306959, 2306960, 2306961, 2306284, 2306287, 2306956, 2306957, 2306962, 2306963, 2306964, and 2306966 contain the supplementary crystallographic data for this paper. These data can be obtained free of charge via www.ccdc.cam.ac.uk/data_request/cif, or by emailing data_request@ccdc.cam.ac.uk, or by contacting The Cambridge Crystallographic Data Centre, 12 Union Road, Cambridge CB2 1EZ, UK; fax:+441223336033. Correspondence and requests for materials should be addressed to B.D. (barun.dhara@riken.jp) or G.W. (go0325@kitasato-u.ac.jp) or D.M. (daigo.miyajima@riken.jp).

Conflict of interest

The authors declare no conflict of interest.

Acknowledgements

The computations were partially performed at the Research Center for Computational Science, Okazaki, Japan (Project: 22-IMS- C043 and 23-IMS-C038). This study was supported by the JSPS KAKENHI (Grant Nos. JP21K18899, JP22K18953, JP24KJ1922), JST PRESTO (Grant No. JP1159382), and CREST (Grant No. JPMJCR23O1). Additional support was provided by the Guangdong Basic Research Center of Excellence for Aggregate Science and the National Natural Science Foundation of China (Grant No. 52272056).

Keywords: Chirality • Polarity • Crystal engineering • Bowl-shaped molecules

Author Contributions

‡These authors contributed equally.

References

1. Nakamura, M.; Horiuchi, S.; Kagawa, F.; Ogawa, N.; Kurumaji, T.; Tokura, Y.; Kawasaki, M., Shift current photovoltaic effect in a ferroelectric charge-transfer complex. *Nat. Commun.* **2017,** *8* (1), 281.

2. Tan, L. Z.; Zheng, F.; Young, S. M.; Wang, F.; Liu, S.; Rappe, A. M., Shift current bulk photovoltaic effect in polar materials—hybrid and oxide perovskites and beyond. *npj Comput. Mater.* **2016,** *2* (1), 1-12.

3. Chiesa, A.; Privitera, A.; Macaluso, E.; Mannini, M.; Bittl, R.; Naaman, R.; Wasielewski, M. R.; Sessoli, R.; Carretta, S., Chirality-Induced Spin Selectivity: An Enabling Technology for Quantum Applications. *Adv. Mater.* **2023,** *35* (28), e2300472.

4. Naaman, R.; Paltiel, Y.; Waldeck, D. H., Chiral Molecules and the Spin Selectivity Effect. *The journal of physical chemistry letters* **2020,** *11* (9), 3660-3666.

5. Aizawa, H.; Sato, T.; Maki-Yonekura, S.; Yonekura, K.; Takaba, K.; Hamaguchi, T.; Minato, T.; Yamamoto, H. M., Enantioselectivity of discretized helical supramolecule consisting of achiral cobalt phthalocyanines via chiral-induced spin selectivity effect. *Nat. Commun.* **2023,** *14* (1), 4530.

6. Pop, F.; Zigon, N.; Avarvari, N., Main-Group-Based Electro- and Photoactive Chiral Materials. *Chem. Rev.* **2019,** *119* (14), 8435-8478.

7. Labella, J.; Bhowmick, D. K.; Kumar, A.; Naaman, R.; Torres, T., Easily processable spin filters: exploring the chiral induced spin selectivity of bowl-shaped chiral subphthalocyanines. *Chem. Sci.* **2023,** *14* (16), 4273-4277.

8. Long, G.; Sabatini, R.; Saidaminov, M. I.; Lakhwani, G.; Rasmita, A.; Liu, X.; Sargent, E. H.; Gao, W., Chiral-perovskite optoelectronics. *Nat. Rev. Chem.* **2020,** *5* (6), 423-439.

9. Zhang, Y.-Y.; Yu, J.-T.; Li, B.; Li, D.-J.; Gu, Z.-G.; Sun, X.-F.; Cai, H.-L.; Kostakis, G. E.; Peng, G., Chiral and kryptoracemic Dy(iii) complexes with field-induced single molecule magnet behavior. *CrystEngComm* **2018,** *20* (32), 4582-4589.

10. Zhang, C.; Guo, Y.; He, D.; Komiya, J.; Watanabe, G.; Ogaki, T.; Wang, C.; Nihonyanagi, A.; Inuzuka, H.; Gong, H.; Yi, Y.; Takimiya, K.; Hashizume, D.; Miyajima, D., A Design Principle for Polar Assemblies with C_3 -Sym Bowl-Shaped pi-Conjugated Molecules. *Angew. Chem., Int. Ed.* **2021,** *60* (6), 3261-3267.

11. Saito, M.; Shinokubo, H.; Sakurai, H., Figuration of bowl-shaped π-conjugated molecules: properties and functions. *Mater. Chem. Front.* **2018,** *2* (4), 635-661.

12. Labella, J.; Lavarda, G.; Hernández-López, L.; Aguilar-Galindo, F.; Díaz-Tendero, S.; Lobo-Checa, J.; Torres, T., Preparation, Supramolecular Organization, and On-Surface Reactivity of Enantiopure Subphthalocyanines: From Bulk to 2D-Polymerization. *J. Am. Chem. Soc.* **2022,** *144* (36), 16579-16587.

13. Mebs, S.; Weber, M.; Luger, P.; Schmidt, B. M.; Sakurai, H.; Higashibayashi, S.; Onogi, S.; Lentz, D., Experimental electron density of sumanene, a bowl-shaped fullerene fragment; comparison with the related corannulene hydrocarbon. *Org. Biomol. Chem.,* **2012,** *10* (11), 2218-2222.

14. Amaya, T.; Seki, S.; Moriuchi, T.; Nakamoto, K.; Nakata, T.; Sakane, H.; Saeki, A.; Tagawa, S.; Hirao, T., Anisotropic Electron Transport Properties in Sumanene Crystal. *J. Am. Chem. Soc.* **2009,** *131* (2), 408-409.

15. González-Rodríguez, D.; Torres, T.; Olmstead, M. M.; Rivera, J.; Herranz, M. Á.; Echegoyen, L.; Castellanos, C. A.; Guldi, D. M., Photoinduced Charge-Transfer States in Subphthalocyanine−Ferrocene Dyads. *J. Am. Chem. Soc.* **2006,** *128* (33), 10680-10681.

16. Duan, C.; Guzmán, D.; Colberts, F. J. M.; Janssen, R. A. J.; Torres, T., Subnaphthalocyanines as Electron Acceptors in Polymer Solar Cells: Improving Device Performance by Modifying Peripheral and Axial Substituents. *Chem. Eur. J.* **2018,** *24* (24), 6339-6343.

17. Brock, C. P.; Schweizer, W. B.; Dunitz, J. D., On the validity of Wallach's rule: on the density and stability of racemic crystals compared with their chiral counterparts. *J. Am. Chem. Soc.* **1991,** *113* (26), 9811-9820.

18. Zhang, X.; Chen, Z.; Liu, X.; Hanna, S. L.; Wang, X.; Taheri-Ledari, R.; Maleki, A.; Li, P.; Farha, O. K., A historical overview of the activation and porosity of metal–organic frameworks. *Chem. Soc. Rev.* **2020,** *49* (20), 7406-7427.

19. Ma, J.; Kalenak, A. P.; Wong-Foy, A. G.; Matzger, A. J., Rapid Guest Exchange and Ultra-Low Surface Tension Solvents Optimize Metal–Organic Framework Activation. *Angew. Chem., Int. Ed.* **2017,** *56* (46), 14618-14621.

20. Okamoto, T.; Kumagai, S.; Fukuzaki, E.; Ishii, H.; Watanabe, G.; Niitsu, N.; Annaka, T.; Yamagishi, M.; Tani, Y.; Sugiura, H.; Watanabe, T.; Watanabe, S.; Takeya, J., Robust, high-performance n-type organic semiconductors. *Science advances* **2020,** *6* (18), eaaz0632.

21. Desiraju, G. R.; Gavezzotti, A., Crystal structures of polynuclear aromatic hydrocarbons. Classification, rationalization and prediction from molecular structure. *Acta Cryst. B* **1989,** *45* (5), 473-482.

22. Goddard, R.; Haenel, M. W.; Herndon, W. C.; Krueger, C.; Zander, M., Crystallization of Large Planar Polycyclic Aromatic Hydrocarbons: The Molecular and Crystal Structures of Hexabenzo[bc,ef,hi,kl,no,qr]coronene and Benzo[1,2,3-bc:4,5,6-b'c']dicoronene. *J. Am. Chem. Soc.* **1995,** *117* (1), 30-41.

23. Mattheus, C. C.; Dros, A. B.; Baas, J.; Meetsma, A.; Boer, J. L. d.; Palstra, T. T. M., Polymorphism in pentacene. *Acta Cryst. C* **2001,** *57* (8), 939-941.

24. Gardberg, A. S.; Yang, S.; Hoffman, B. M.; Ibers, J. A., Synthesis and Structural Characterization of Integrally Oxidized, Metal-Free Phthalocyanine Compounds: [H2(pc)][IBr2] and [H2(pc)]2[IBr2]Br·C10H7Br. *Inorg. Chem.* **2002,** *41* (7), 1778-1781.

25. Rodríguez-Morgade, M. S.; Claessens, C. G.; Medina, A.; González-Rodríguez, D.; Gutiérrez-Puebla, E.; Monge, A.; Alkorta, I.; Elguero, J.; Torres, T., Synthesis, Characterization, Molecular Structure and Theoretical Studies of Axially Fluoro-Substituted Subazaporphyrins. *Chem. - Eur. J.* **2008,** *14* (4), 1342-1350.

26. Jin, Z.; Teo, Y. C.; Zulaybar, N. G.; Smith, M. D.; Xia, Y., Streamlined Synthesis of Polycyclic Conjugated Hydrocarbons Containing Cyclobutadienoids via C–H Activated Annulation and Aromatization. *J. Am. Chem. Soc.* **2017,** *139* (5), 1806-1809.

27. Fulford, M. V.; Jaidka, D.; Paton, A. S.; Morse, G. E.; Brisson, E. R. L.; Lough, A. J.; Bender, T. P., Crystal Structures, Reaction Rates, and Selected Physical Properties of Halo-Boronsubphthalocyanines (Halo = Fluoride, Chloride, and Bromide). *J. Chem. Eng. Data* **2012,** *57* (10), 2756-2765.

28. Lawton, R. G.; Barth, W. E., Synthesis of corannulene. *J. Am. Chem. Soc.* **1971,** *93* (7), 1730-1745.

29. Yong, T.; Báti, G.; García, F.; Stuparu, M. C., Mechanochemical transformation of planar polyarenes to curved fused-ring systems. *Nat. Commun.* **2021,** *12* (1), 5187.

30. Schmidt , B. M.; Topolinski , B.; Yamada , M.; Higashibayashi, S.; Shionoya, M.; Sakurai, H.; Lentz, D., Fluorinated and Trifluoromethylated Corannulenes. *Chem. Eur. J.* **2013,** *19* (41), 13872-13880.

31. Wu, Y.-T.; Bandera, D.; Maag, R.; Linden, A.; Baldridge, K. K.; Siegel, J. S., Multiethynyl Corannulenes: Synthesis, Structure, and Properties. *J. Am. Chem. Soc.* **2008,** *130* (32), 10729-10739.

32. Tian, X.; Xu, J.; Baldridge, K. K.; Siegel, J. S., Fluorous Corannulenes: Ab initio Predictions and the Synthesis of sym-Pentafluorocorannulene. *Angew. Chem. Int. Ed.* **2020,** *59* (4), 1460-1464.

33. Kise, K.; Ooi, S.; Osuka, A.; Tanaka, T., Five-fold-symmetric Pentabromo- and Pentaiodo-corannulenes: Useful Precursors of Heteroatom-substituted Corannulenes. *Asian J. Org. Chem.* **2021,** *10* (3), 537-540.

Figures and figure legends

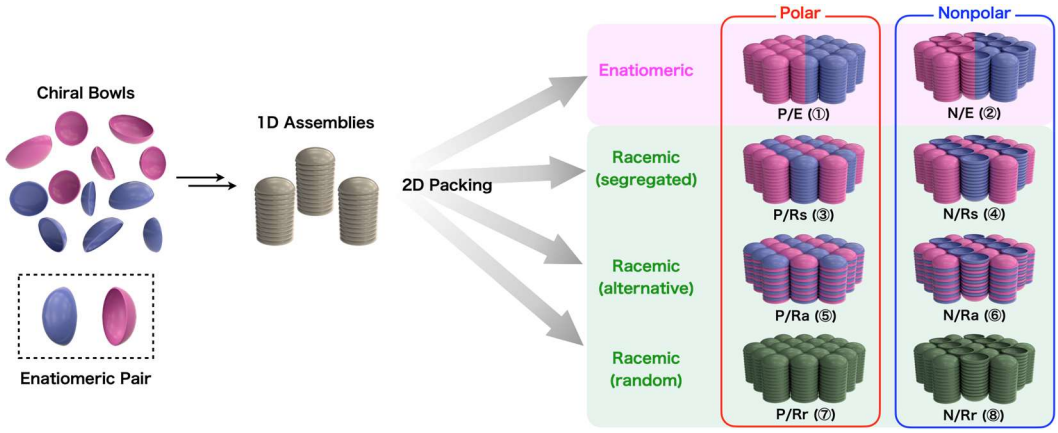

Figure 1 | Schematic illustration of possible two-dimensional packings of columns consisting of chiral bowl-shaped molecules.

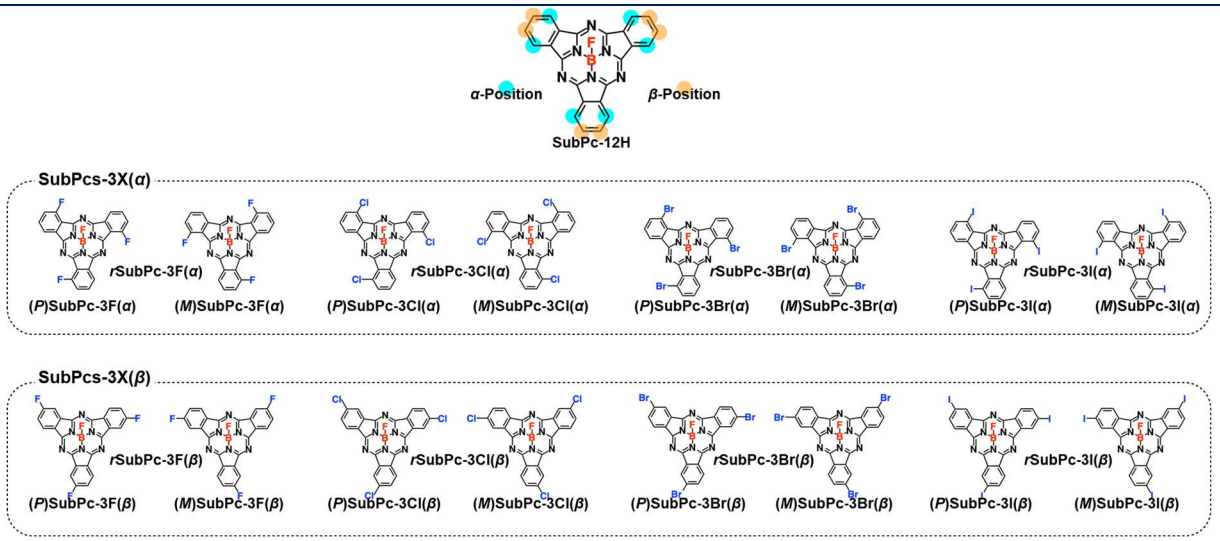

Figure 2 |Chemical structures of chiral subphthalocyanine (SubPc) derivatives together with a schematic illustration of the α- and β-positions of SubPc.

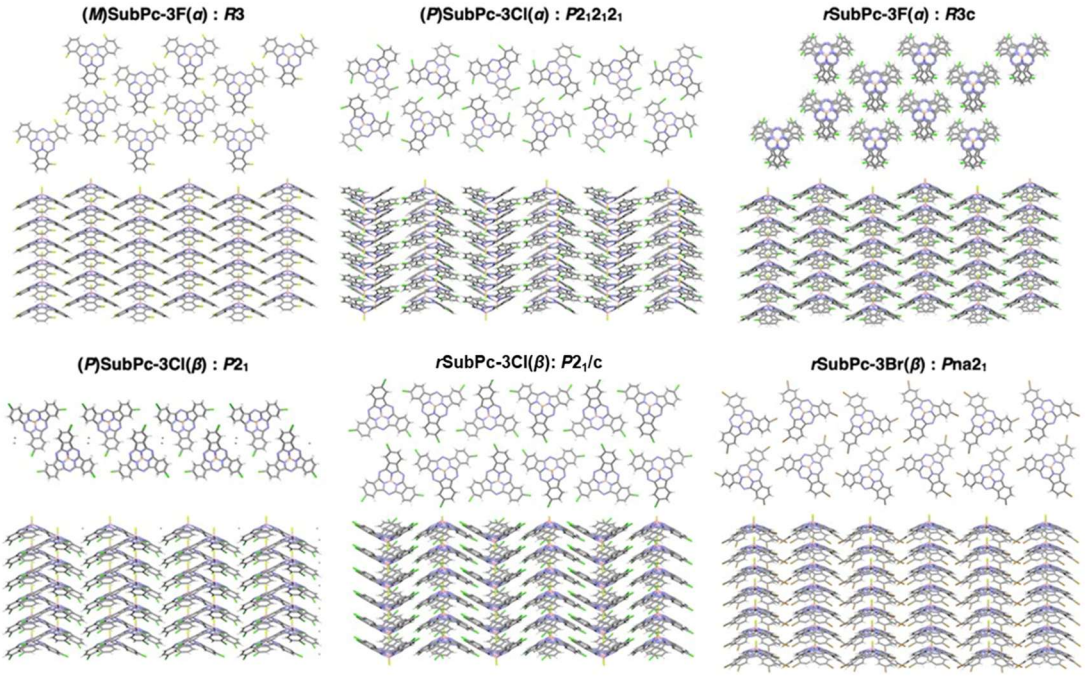

Figure 3 | Schematic illustrations of representative molecular packings of SubPc derivatives. Other crystals are summarized in Figure S27.

Table 1. The summary of the space groups of SubPc derivatives. ①–⑧ correspond to the molecular arrangements discussed in Figure 1.

	α		β	
	Enantiopure	Racemic	Enantiopure	Racemic
F	*R*3(①)	*R*3m(⑦)	$P2_12_12_1$(②)	$P2_12_12_1$(⑧)
Cl	$P2_12_12_1$(②)	*R*3c(⑤)	$P2_1$	$P2_1/c$(④)
Br	$P2_12_12_1$(②)	*R*3c(⑤)	$P2_1$	$Pna2_1$(③)
I	$P2_12_12_1$(②)	*R*3c(⑤)	*C*2	$Pna2_1$(③)

Polar (parallel) / Non-Polar (anti-parallel) / Polar (parallel) with MeOH

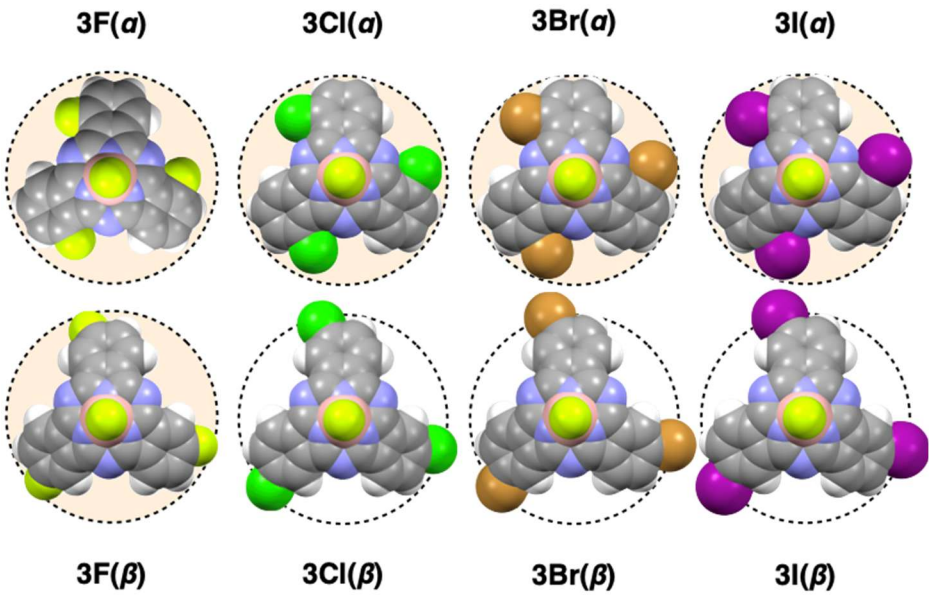

Figure 4 | Top-view images of SubPc derivatives based on their corresponding single crystal data. The same dashed circular lines, corresponding to the peripheral of non-substituted SubPc, are placed to compare the sizes. SubPcs on top of orange circles correspond to the crystals in orange cells in Table1.

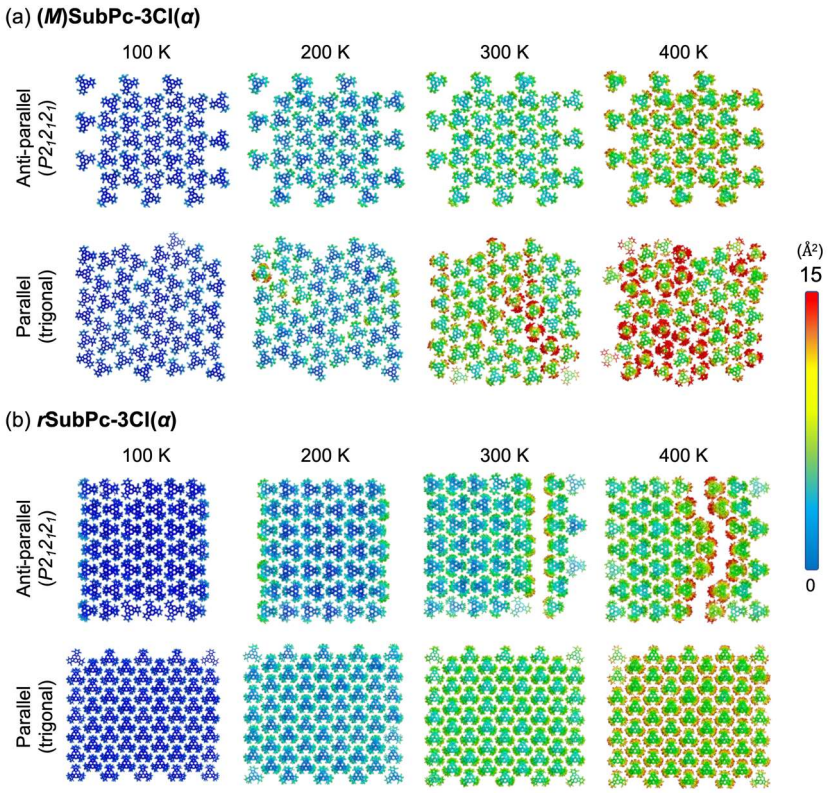

Figure 5 | Color-coded *B*-factor distributions (Å^2) obtained from MD simulations for (a) (*M*)SubPc-3Cl(*α*) and (b) *r*SubPc-3Cl(*α*). The magnitude of *B*-factors is represented by the color-coded scale bar.